J|A|C|S
ARTICLES
Published on Web 05/25/2002

Phospholipid/Protein Cones

Bijaya K. Mishra and Britt N. Thomas*

Contribution from the Department of Chemistry, Louisiana State University, Baton Rouge, Louisiana 70808

Received January 14, 2002

Abstract: The presence of protein in tubule-forming solutions of the diacetylenic phospholipid 1,2-bis-(10,12-tricosadiynoyl)-*sn*-glycero-3-phosphocholine results in the formation of hollow cones rather than the expected hollow cylinders. Differential phase-contrast video microscopy reveals that cones grow from proteinaceous nodules in a fashion similar to cylindrical tubule growth from spherical vesicles. Spatially resolved electron-beam energy-dispersive X-ray fluorescence spectroscopy shows the protein to be associated with the cone wall. Small-angle X-ray scattering shows that, like the protein-free cylinders, the cones are multilamellar with essentially identical interlamellar spacing.

Introduction

Diynes placed midway in the long hydrocarbon tails of lecithins such as dimyristoylphosphatidylcholine (DMPC) or dipalmitoylphosphatidylcholine (DPPC) enable the robust self-assembly of tubules: stable, hollow crystalline vesicles with a cylindrical morphology, as first reported by Yager and co-workers.[1−4] The solvent in which tubules assemble influences their morphology: the prototypical tubule-forming molecule, 1,2-bis(10,12-tricosadiynoyl)-*sn*-glycero-3-phosphocholine (hereafter "DC(8,9)PC," Figure 1) produces unilamellar cylinders of dimension $\approx$0.5 μm $\times$ $\approx$15 μm in methanolic solutions,[5] but in ethanolic solutions the tubules consist of some four to eight coaxially nested cylinders of dimension $\approx$0.55 μm $\times$ $\approx$25 μm, with an interlamellar spacing $d = 65$ Å.[5] Furthermore these "ethanolic" cylinders display a helical trace on their exteriors, a remnant of an intermediate structure, a helically wound bilayer ribbon whose normal is perpendicular to the cylinder axis. This helically wound ribbon subsequently widens to form closed cylinders.[6] The sensitivity of tubule formation to solvent environment is further demonstrated by the next alcohol in the series; in propanolic solutions tubule formation ceases with the "corkscrew" helical intermediate.[7]

Tubule hollowness suggests medical[8] and industrial encapsulation applications.[9−11] Stringent control of tubule morphology will be required to optimize tubules for these uses. For example, while adjusting the amount of encapsulant delivered is a simple matter of changing the number of tubules dispensed, some properties, such as the encapsulant time-release profile, are expected to depend intimately upon tubule length and diameter. Another important property determined by tubule morphology is the mean deposition distance of aerosolized tubules subjected to shear flow, the conditions of aerosol therapy.[12] Under these conditions, tubule diameter dominates the particle mean deposition distance, and so regulation of tubule diameter is required to control where medicine-laden tubules will deposit in the respiratory tract.

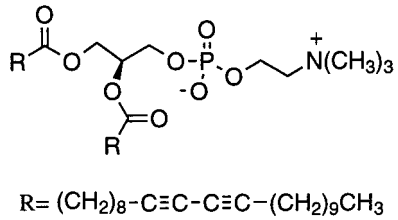

Figure 1. The *S*-enantiomer of the diynoic phospholipid DC(8,9)PC.

The simplest approach to filling these microscopic cylinders is to prepare them in an encapsulant-rich solution, thereby enveloping dissolved encapsulant in the cylinder void.[13] Given tubules' sensitivity to their solvent environment, however, it is important to ask what effects dissolved encapsulant might exert upon tubule morphology. A relatively small fungicidal molecule has already been studied,[13] and we have therefore chosen to study the effects that a large molecule, such as a protein, might have upon tubule morphology.

A widely used tubule formation protocol is to place DC(8,9)PC in an ethanol:water solvent system, typically 0.75:0.25 (v:v), and heat to approximately 50 °C to dissolve

* Corresponding author. E-mail: bthomas@lsu.edu.

(1) Schoen, P. E.; Yager, P.; Priest, R. G. *NATO ASI Ser., Ser. E* **1985**, *102* (Polydiacetylenes), 223−232.
(2) Yager, P.; Schoen, P. E.; Davies, C.; Price, R.; Singh, A. *Biophys. J.* **1985**, *48*, 899−906.
(3) Schoen, P. E.; Yager, P. *J. Polym. Sci., Polym. Phys. Ed.* **1985**, *23*, 2203−2216.
(4) Yager, P.; Schoen, P. E. *Mol. Cryst. Liq. Cryst.* **1984**, *106*, 371−381.
(5) Ratna, B. R.; Baral-Tosh, S.; Kahn, B.; Schnur, J. M.; Rudolph, A. S. *Chem. Phys. Lipids* **1992**, *63*, 47−53.
(6) Thomas, B. N.; Lindemann, C. M.; Clark, N. A. *Phys. Rev. E* **1999**, *59*, 3040−3047.
(7) Georger, J. H.; Singh, A.; Price, R. R.; Schnur, J. M.; Yager, P.; Schoen, P. E. *J. Am. Chem. Soc.* **1987**, *109*, 6169−6175.
(8) Johnson, D. L.; Polikandritou-Lambros, M.; Martonen, T. B. *Drug Delivery* **1996**, *3*, 9−15.
(9) Schnur, J. M. *Science* **1993**, *262*, 1669−1676.
(10) Archibald, D. D.; Mann, S. *Chem. Phys. Lipids* **1994**, *69*, 51−64.
(11) Baum, R. *Chem. Eng. News* **1993**, *August 9*, 19−20.
(12) Johnson, D. L.; Esmen, N. A.; Carlson, K. D.; Pearce, T. A.; Thomas, B. N. *J. Aerosol. Sci.* **2000**, *31*, 181−188.
(13) Price, R.; Patchan, M. *J. Microencapsulation* **1991**, *8*, 301−306.

10.1021/ja020067h CCC: $22.00

the DC(8,9)PC. As the solution slowly cools to room temperature, multilamellar spherical vesicles form, and finally tubules erupt from these vesicles and precipitate. To study the perturbative effects a protein might exert on tubule formation, we have chosen to modify this protocol minimally by adding small amounts of protein to the ethanol:water:lipid mixture prior to heating. We expect nearly all proteins to be random coils at the ethanol concentrations employed, and take the näive stance for this initial study that protein features such as charge and hydrophobicity will be relatively unimportant under these conditions. We have selected the inexpensive, readily available protein lysozyme for this study.

Experimental Section

(a) Specimen Preparation. Thermal cycle: A 1 mg sample of DC(8,9)PC (Figure 1) was dispersed in 1 mL of a 90:10 (v:v) mixture of reagent-grade ethanol and 18 M·ohm water mixture at room temperature by vigorous stirring. This ethanol:water ratio is higher than our usual 0.75:0.25 ratio, and was chosen to facilitate solvent evaporation during electron microscopy specimen preparation, rather than for protein solubility reasons. This change did not affect tubule yield appreciably. As expected, the solution became turbid upon cooling to room temperature and eventually a flocculent precipitate formed. Optical microscopic examination showed the precipitate to consist solely of the expected cylindrical tubules. This "stock" dispersion was stored at subzero temperature. A 1 mg sample of lysozyme (14 kDalton, from chicken egg white, Sigma Chemical) was then added to 1 mL aliquots of the lipid stock dispersion, with stirring, and this homogeneous lipid/protein dispersion was subjected to the standard tubule formation thermal cycle, i.e., heating the dispersion to clarity (about 55 °C) with vigorous stirring and cooling to room temperature at 0.1 ± 0.02 °C per min. The resultant milky solution and precipitate, which we will demonstrate is predominantly microscopic cones, was also refrigerated after reaching room temperature.

The possibility that the lysozyme distorts already-formed tubules was eliminated by examining lysozyme-containing aliquots *not* subjected to the thermal cycle. These specimens were otherwise treated in the same manner as those subjected to the thermal cycle, except vastly greater exposure time to the lysozyme was allowed. Microscopic examination revealed only undistorted cylindrical tubules to be present, along with a granular precipitate indistinguishable from that found in thermally cycled lipid-free lysozyme solutions.

(b) Physical Characterization. The precipitate was examined with Nomarksi Differential Interference Contrast (DIC) video microscopy, scanning electron microscopy (SEM) and transmission electron microscopy (STM), energy-dispersive X-ray fluorescence (EDX), small-angle X-ray scattering (SAXS), and contact-mode atomic force microscopy (AFM).

Optical Microscopy. A drop of homogeneous dispersion was taken from the flask after vigorous stirring, placed upon a glass slide, and covered with a cover slip, the edges of which were sealed with a fast-drying cyanoacrylate glue to suppress solvent evaporation. Utmost care was taken to not allow the glue to spread between the slide and cover slip. After optical examination, these samples were subjected to another tubule-formation thermal cycle while being monitored with Nomarski DIC video microscopy to observe "real-time" structural transitions.

Electron Microscopy and Energy-Dispersive X-ray Fluorescence Spectroscopy. Scanning and transmission electron microscopy specimens were prepared similarly, namely, a drop of homogeneous dispersion was placed upon the appropriate standard conductive carbon substrate, which in turn was placed on an aluminum stub, air-dried under ambient conditions, finally producing the expected thin, waxy film. Some scanning electron microscopy specimens were coated with a standard gold/palladium mixture (Au:Pd 80:20) under vacuum in an Edwards S150 sputter coater before being examined, while others were evaporatively carbon-coated in a Balzers MED-010 vacuum evaporator. All specimens were observed with a Cambridge Stereoscan 260 SEM at acceleration voltages between 5 and 20 keV, typically at 15 keV. Because the solvent and lipid are sulfur-free, while the protein is not, energy-dispersive X-ray fluorescence (EDX) was used for determining sulfur distribution with the goal of ascertaining protein distribution along the conical structure. It was first determined by EDX that the electron microscopy substrates either were sulfur-free (the bare metal stubs) or had a negligibly small sulfur signal (the carbon-coated stubs). Electron diffraction patterns and dark field and high-resolution TEM images were taken with a JEOL JEM 2010 electron microscope operated at 200 keV with a point-to-point resolution of 2.3 Å.

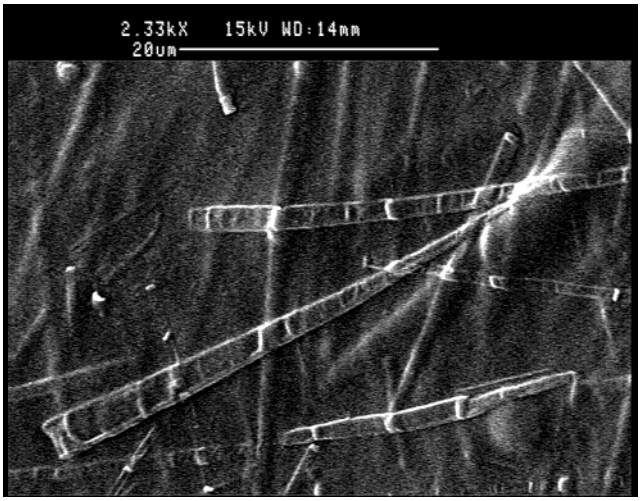

Figure 2. Scanning electron micrograph of phospholipid/protein cones lying atop a dried bed of the lysozyme/DC(8,9)PC mixture.

Atomic Force Microscopy. Atomic force microscopy specimens were prepared by placing a small aliquot of the stirred protein/lipid dispersion upon a glass slide, which was then spread about the slide by tilting. A thin waxy film resulted after air-drying under ambient conditions, which was probed by contact-mode AFM with a silicon nitride cantilever tip in a vibration and acoustically isolated hutch.

Small-Angle X-ray Scattering. Small-angle X-ray scattering was conducted at beamline X10A of the National Synchrotron Light Source at Brookhaven National Laboratory. A monochromatized 1.6009 Å X-ray beam was defined by 0.3 mm (vertical) × 10 mm (horizontal) slits in the incident and diffracted beampaths, yielding a measured in-plane resolution of 0.0015 $Å^{-1}$ (fwhm). To enhance scattering signal, concentrated samples of $c \approx 100$ mg lipid/mL were prepared by centrifuging the $c \approx 1$ mg lipid/mL dispersion on a benchtop centrifuge for 5 min. (Optical microscopy of tubules centrifuged at a much higher 10000*g* centrifugation at 20 °C for 30 min revealed no discernible change in tubule morphology.[14]) The concentrated paste was placed in standard 1.5 mm diameter quartz diffraction capillaries, yielding unoriented powder samples. The specimen was translated an integral number of times through the X-ray beam during data acquisition to minimize the effects of radiation damage[14] as scattering was collected over 0.001 $Å^{-1} \leq |k| \leq 0.060$ $Å^{-1}$ at ambient temperature.

Results

Scanning-Mode Electron Microscopy (SEM). Electron microscopy shows that precipitates from lysozyme-containing DC(8,9)PC solutions are composed primarily of conical tubules, with a small number of undistorted cylindrical tubules present, as shown in Figure 2. Under the conditions of this study,

(14) Thomas, B. N.; Safinya, C. R.; Plano, R. J.; Clark, N. A. *Science* **1995**, *267*, 1635−1638.

cylinders were comparatively rare, in marked contrast to protein-free DC(8,9)PC specimens, which contain only cylinders.

Energy-Dispersive X-ray Fluorescence. The cones exhibit helical ridges on their exteriors that are similar to, but more pronounced than, those found on undistorted cylinders, as seen in Figure 2. This difference suggests that a compositional inhomogeneity might exist at the cones' ridges, e.g., they might be protein-rich with respect to the remainder of the cone. Because the solvents, tubule-forming molecule, and the substrate are sulfur-free, while the protein contains sulfur-bearing residues, Energy Dispersive X-ray fluorescence (EDX) was used to map sulfur concentration as a probe of relative protein density. No significant protein concentration modulation along the cone's length was detected by EDX. A very slight depression in sulfur fluorescence was found at the ridges, but this difference is very small with respect to our counting statistics. In contrast, sulfur fluorescence from cones is significantly higher than adjacent solution-covered substrate. This difference indicates protein association with the lipid. It is important to keep in mind that lysozyme is not a protein usually associated with membrane physiology, and further, under our conditions it is certainly a random coil.

Transmission-Mode Electron Microscopy (TEM). Transmission-mode electron microscopy (TEM) probes were conducted to augment the SEM results for three reasons. First, SEM is a surface-sensitive probe, and our conclusion that cones dominate could be incorrect if, for some reason, cones are found preferentially at the specimen surface. That is, the specimen's transparency to TEM can verify the cones' predominance. Second, the SEM specimen preparation involves subjecting the specimen to high vacuum and spallating metallic ions onto the specimen surface, whereas the TEM protocol involves only the high-vacuum step. While protein-free tubules are known to survive the SEM preparation protocol, the possibility of artifact induction in the protein/lipid system by the SEM specimen preparation protocol can essentially be eliminated if corroborating results are provided by TEM. Finally, TEM generally permits higher magnification.

The coexistence of conical tubules in the bulk and their predominance is confirmed clearly in Figure 3, a lipid/protein specimen TEM micrograph. The dispersity in cone length and the haphazard formation of a random netlike matrix as the tubule dispersion dries is also evident.

Optical Microscopy. Tubules are known to form by at least two mechanism: (1) growth from cooling spherical vesicles and (2) directly from solution through the isothermal addition of water to the ethanolic solution, which decreases lipid solubility. In situ Nomarski DIC optical microscopy movies of the first mechanism can been made,[6] and Figure 4 is the result of applying this technique to cone formation.

At first glance the processes are remarkably similar: in both systems the structures form as helically wound ribbons growing at about 1 μm/s from large objects. Indeed, the primary difference between protein-free tubule and protein-mediated cone formation is the substitution of granular nodules for lipid vesicles in the proteinaceous solution as the growth site. (We surmise these particles are primarily protein, for they appear only in lysozyme-containing solutions as they pass through $\approx$54 °C in the cooling cycle.)

(15) Reference deleted in press.

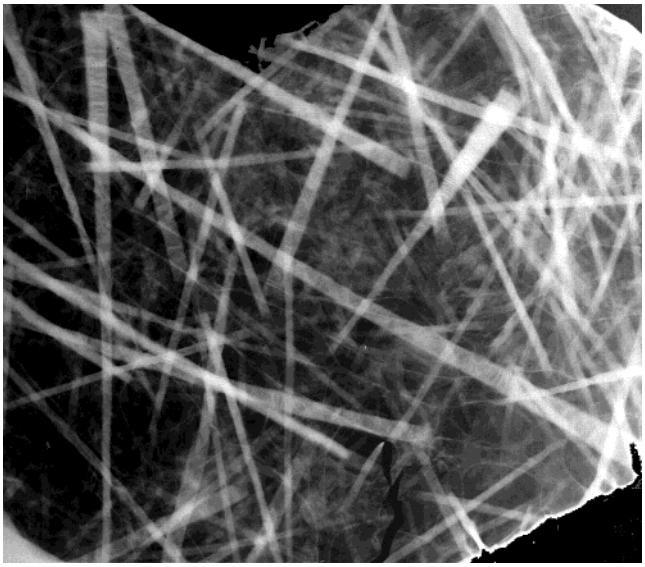

Figure 3. Transmission electron micrograph of an air-dried lysozyme/DC-(8,9)PC mixture, showing coexisting cones and cylinders forming an entangled network.

Another fundamental difference is that protein-free tubules cycle reversibly to spherical vesicles when reheated above the chain-melting temperature, but there is no corresponding cone-to-vesicle transition in the protein-containing system. Upon heating, cones appear to dissolve; spherical vesicles either do not form as cones melt, as they do in protein-free systems,[6] or the vesicles are smaller than the $\approx$0.25 μm resolving power of the optical microscope. Interestingly, cones reappear upon subsequent recooling. The formation temperatures are different as well: cone growth begins at approximately 50 °C, while in protein-free DC(8,9)PC solutions the vesicle-to-tubule transition occurs at $\approx$39 °C. Finally, a difference that unfortunately is not evident in the static frames of Figure 4 is an undulation that occurs along the forming cone's axis that does not occur in forming tubules. This "wiggle" suggests the cone is not as rigid as protein-free tubules, a point we investigate with atomic force microscopy.

Atomic Force Microscopy. The cone's apparent deformability was investigated with atomic force microscopy (AFM). AFM studies of tubules made from phosphonate analogues of DC(8,9)PC revealed them to be so deformable that upon air-drying they flattened to a height of about four bilayers.[16,17] Contact-mode AFM performed upon cones gave the same result, namely, air-dried cones' cross-sections are not circular, but rectangular with a height of about four bilayers.

Small-Angle X-ray Scattering. The membranes composing cones and tubules are multilamellar, and small-angle X-ray scattering (SAXS) was used to compare this common feature. The interlamellar (00l) fundamental peaks for the DC(8,9)PC tubules and cones were found to be centered at $|k_0| = 4\pi \sin(2\theta/2)/\lambda = 0.0971$ and 0.0949 Å^{-1}, respectively, implying interlamellar spacings d of 64.7 and 66.2 Å, respectively (see Figure 5). In view of the morphological differences between tubules and cones, we interpret this small change as an indication

(16) Thomas, B. N.; Corcoran, R. C.; Cotant, C. L.; Lindemann, C. M.; Kirsch, J. E.; Persichini, P. J. *J. Am. Chem. Soc.* **1998**, *120*, 12178−12186.
(17) Thomas, B. N.; Corcoran, R. C.; Cotant, C. L.; Lindemann, C. M.; Kirsch, J. E.; Persichini, P. J. *J. Am. Chem. Soc.* **2002**, *124*, 1227−1233.

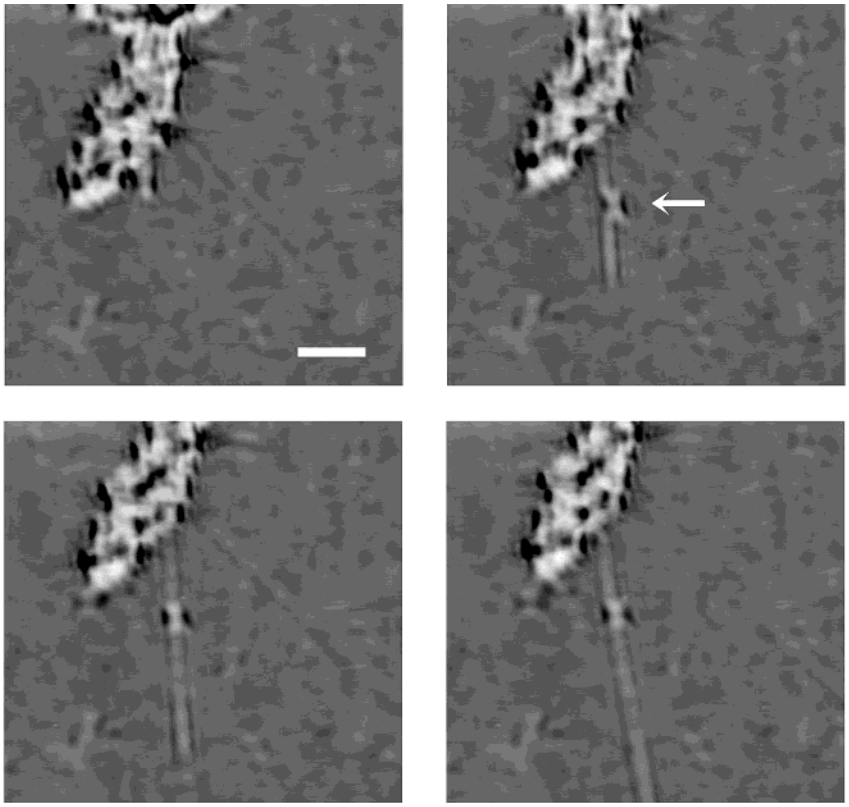

Figure 4. Four Nomarski DIC microscopy video frames, separated by 5 s, of cone formation occurring in a phospholipid/protein solution cooling at 0.25 °C/h. The granular particle does not appear to change in size, with the exception of a piece that appears to have broken off, indicated by the arrow in the second frame. The cone vertex is at the granular nodule. The scale bar is 5 μm long.

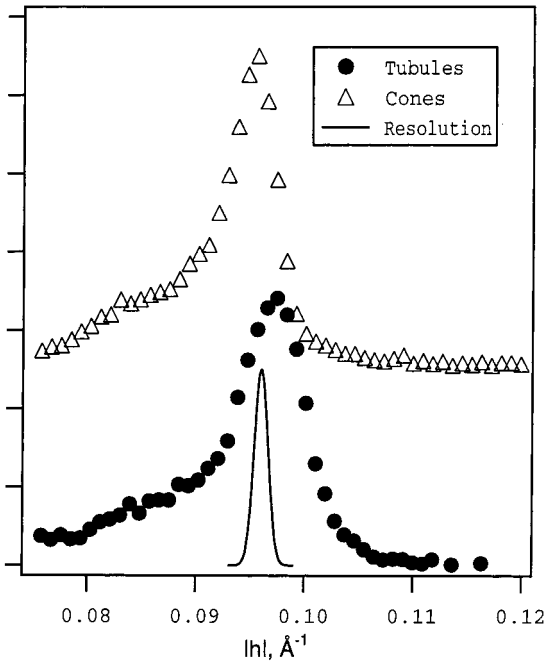

Figure 5. Small-angle X-ray scattering from protein-free DC(8,9)PC tubules and protein-mediated DC(8,9)PC cones. The traces are shifted vertically for clarity. The protein-free tubule (00*l*) peak is centered at 0.0971 Å^{-1}, indicating an interlamellar spacing of 64.7 Å, and the protein/cone peak is centered at 0.0949 Å^{-1}, indicating an interlamellar spacing of 66.2 Å. The error bars are smaller than the symbols. The solid curve is the 0.0015 Å^{-1} fwhm instrument resolution.

of the dominance of interlamellar forces in comparison to those that distort forming tubules into cones.

Interestingly, conical specimens generated no reflections over the range 0.006 Å^{-1} $\leq |l| \leq$ 0.45 Å^{-1} (roughly speaking, 10 Å $\leq |d| \leq$ 1,000 Å) that were appreciably different from those arising from protein-free tubules. While it is possible cone dimensions and symmetry create an X-ray form factor that suppresses X-ray reflections arising from microscopic proteinaceous structures, their absence in AFM, SEM, TEM, and optical microscopy probes in conjunction with the small interlamellar spacing perturbation suggests such structures do not exist.

Conclusions

We report the formation of phospholipid cones through the actions of lysozyme added to an otherwise cylinder-forming system, and we find these cones form at substantially higher temperatures than do protein-free tubules. While EDX probes indicate an attractive protein−lipid interaction, the protein's uniform distribution along the highly organized, period conical structure suggests this interaction is weak. A weak interaction is not surprising, for lysozyme is not normally associated with membrane structure, and furthermore, under our conditions it is certainly a denatured random coil. Our observations fail to detect a cone-to-vesicle transformation in protein-containing specimens upon heating, in contrast to the reversible tubule-to-vesicle transition seen in protein-free systems.

A uniform-width helically wound ribbon forms a cylinder when the helical pitch equals the ribbons width, that is, when the ribbon's leading and trailing edges are in contact. When the pitch is less than the ribbon width, subduction of the ribbon's leading edge beneath the trailing edge results in a cone. This is illustrated in Figure 6, where a cone is made from a spiral ribbon by pulling the ribbon end perpendicular to the coil. Continuity

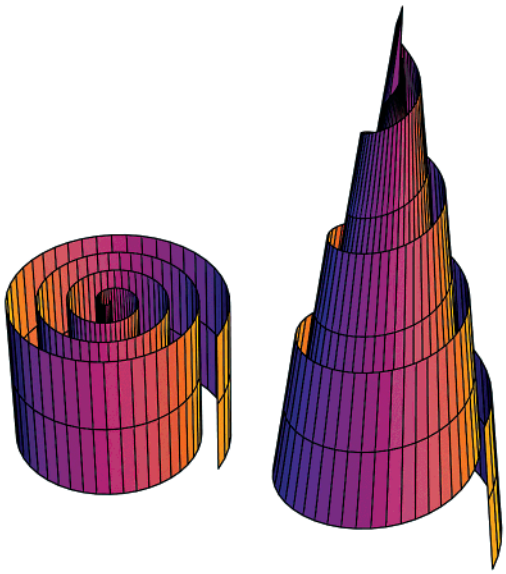

Figure 6. The transformation of a spiral-wound ribbon into a cone. Pulling the internal end of a nonelastic ribbon perpendicular to the plane inhabited by the coil may result in a cone, so long as the ribbon's trailing edge remains subducted beneath its leading edge.

of the cone wall is maintained by sustaining contact of the leading edge with the inner side of the ribbon lying one winding ahead. While it is possible to fashion a "smooth" cone whose leading and trailing edges are in contact, that is, involving no subduction, a ribbon of monotonically increasing width is required. We assume that the simpler edge subduction of a uniform-width ribbon is the mechanism by which cones form.

Very rarely an isolated cone is found among thousands of cylindrical tubules in protein-free DC(8,9)PC preparations.[7] The extreme rarity of cones in protein-free systems and the inability to discover a set of conditions favoring their formation leads to the speculation that these aberrations are the products of chance inhomogeneities in the tubule-forming solution. For instance, it is possible that despite vigorous efforts to maintain sample purity, some sort of contaminant "seed" nucleus generates conical morphology. Another possibility is that mechanical interference, concentration gradients, or other kinetic effects resulting from neighboring nucleation sites' growth creates a local inhomogeneity favoring conical growth. The absence of protein adhering to these rare protein-free tubule exteriors results in dramatically clearer imaging, as shown in the SEM of Figure 7, where leading edge subduction is clearly seen. Of considerable interest is the faint striated pattern running parallel to the ribbon axis, which may be evidence of an internal chiral-tilt defect predicted by Selinger and co-workers.[18,19]

While tubules may serve as chemical or drug encapsulants by forming them in encapsulant-rich solutions, the number of published studies of this potential application is small,[8,20] and none probe the tubule/encapsulant structure. The unexpected conical morphology we observe shows that the encapsulant cannot simply be dismissed as a passive constituent. Indeed, the encapsulant may determine capsule morphology, which in turn will influence application-critical parameters.

For example, the effective aerodynamic diameter of a cone is different than that of a cylinder, and so the mean deposition distance of aerosol-delivered cones in applications such as inhalation therapy[8] will be different than that of similarly sized cylinders.

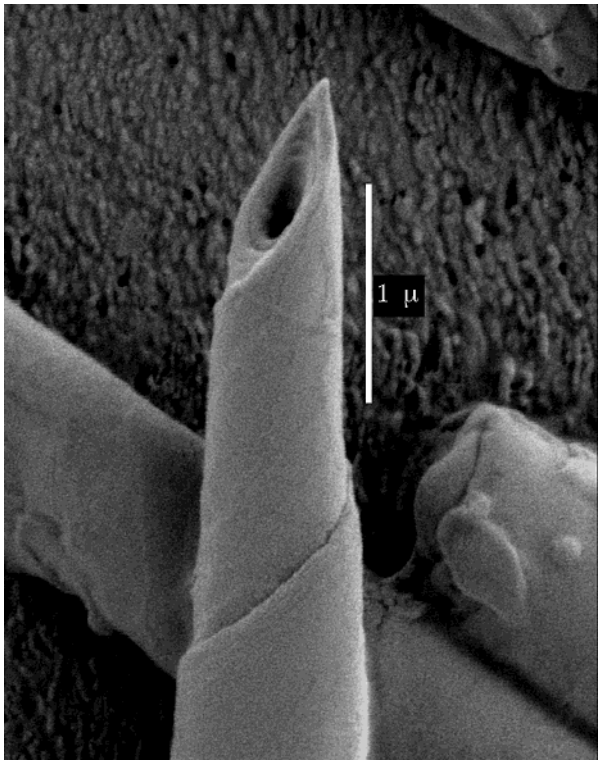

Figure 7. Scanning electron micrograph of a rare protein-free DC(8,9)PC cone. The subduction of the trailing ribbon edge under the leading edge discussed in the text is evident. Note the division of the ribbon into subtle stripes running the ribbon's length.

Another application-critical parameter is the encapsulant time-release profile. Our results suggest significant encapsulant amounts may be integrated into the cone wall's bilayer structure, or otherwise adhering to the cone wall. These bound materials will presumably be released more slowly than "free" encapsulant in the cone's void. In the limits of small quantities of bound material or very low mobility, the effusion of "free" encapsulant from the cone void will dominate the time-release profile. Care must be taken in characterizing the encapsulant morphology, however, for effusion from a cone may differ significantly from that expected from a cylinder by virtue of the cone's effusion occurring at ends of different diameters.

Experimental observations impose the restriction upon tubule structure theory that it predict a cylindrical diameter independent of solvent environment, tubule length, and formation history. Single-component equilibrium theories featuring competition between molecular tilt orientation, chiral packing effects, and membrane elasticity have been quite successful in meeting these experimental conditions.[21] The surprising monotonically increasing diameter resulting from protein mediation and the direct observation of conical growth from the vertex may provide further insight into the delicate balance of forces resulting in tubule formation.

Acknowledgment. B.N.T. was supported by NSF CAREER Grant CHE-9734266. The authors thank Ms. Cindy

(18) Selinger, J. V.; Schnur, J. M. *Phys. Rev. Lett.* **1993**, *71*, 4091−4094.
(19) Selinger, J. V.; MacKintosh, F. C.; Schnur, J. M. *Phys. Rev. E: Stat. Phys., Plasmas, Fluids, Relat. Interdiscip. Top.* **1996**, *53*, 3804−3818.
(20) Schnur, J. M.; Price, R.; Rudolph, A. S. *J. Controlled Release* **1994**, *28*, 3−13.
(21) Kamien, R. D.; Selinger, J. V. *J. Phys.: Condens. Matter* **2001**, *13*, R1−R22.

Henk and Dr. J. C. Jiang of the LSU Biological Sciences and Mechanical Engineering Departments, respectively, for their expert and enthusiastic technical assistance and guidance in the electron microscopy portions of this work. We also thank Dr. Xiaogang Xie of the LSU Geology Department for his invaluable assistance with the EDX probes. Portions of this work were executed at beamline X10A of the National Synchrotron Light Source at Brookhaven National Laboratory, administered by the United States Department of Energy.

JA020067H